RSC Advances

This article can be cited before page numbers have been issued, to do this please use: S. K. Roymuhury, D. Chakraborty and R. V, *RSC Adv.*, 2016, DOI: 10.1039/C6RA09789H.

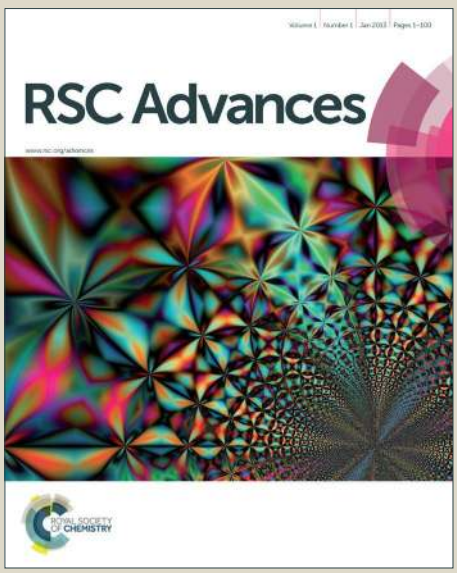

ROYAL SOCIETY OF CHEMISTRY

www.rsc.org/advances

View Article Online
DOI: 10.1039/C6RA09789H

Journal Name

ARTICLE

Zwitterionic niobium and tantalum complexes with bidentate aminophenol scaffolds: Synthesis, structural characterization and use in the ring opening polymerization of lactides

Received 00th January 20xx,
Accepted 00th January 20xx

DOI: 10.1039/x0xx00000x

www.rsc.org/

Sagnik K. Roymuhury,[a] Debashis Chakraborty,*[b] and Venkatachalam Ramkumar[b]

The stoichiometric reaction of the aminophenol ligands **L1**-**L3** with $NbCl_5$ or $TaCl_5$ afforded a series metal chloride complexes **1**-**6**. These were characterized by ^1H, ^{13}C NMR, mass spectroscopy and elemental analysis. Complex **2** crystallized as ethoxy substituted complex **2a** upon attempting crystallization from a solvent mixture of chloroform and ethanol. The molecular structure confirms the zwitterionic nature of the complex where the protonated nitrogen atom of the ligand backbone is neutralised by a negative charge on the metal center. Moderate electrostatic hydrogen bonding interactions between the NH^+ donor moieties and acceptor chlorine atoms stabilise these complexes. The complexes show moderate activities towards the ring opening polymerization (ROP) of lactides (*rac*-LA, *L*-LA) with good control over the polymerization parameters. All the complexes produced heterotactic enriched poly(lactic acid) (PLA). Low molecular weight oligomers prepared and analysed by MALDI-TOF mass and ^1H NMR spectroscopy revealed that the ligand initiates the ROP. The complexes were optimized at B3LYP/LANL2DZ level and the frontier orbitals were studied in order to calculate the trend in reactivity order theoretically.

Introduction

Over the past two decades, poly(lactic acid) (PLA), derived from annually renewable feed stocks such as corn, starch and sugar beet, has received considerable attention because of its potential as an alternative to the conventional polymeric materials based on rapidly depleting petroleum resources.[1] Due to its biodegradability and biocompatibility, PLA finds a broad range of applications in eco-friendly packaging, sophisticated biomedical devices as well as in the pharmaceutical discipline such as carriers for controlled release of drugs, surgical sutures, tissue engineering, stents, medical implants etc.[2] The ring opening polymerization (ROP) of lactide using metal complexes as catalysts is the most convenient synthetic strategy to produce PLAs as this method affords polymers with both high and controlled number average molecular weight (M_n) and narrow molecular weight distributions (MWDs).[3] The two stereogenic centers in lactide monomer are not altered during the ROP. Hence, the stereoselectivity of the catalyst plays a crucial role in determining the tacticity or microstructure of the PLA obtained from *rac*-LA.[4] Significant advances have been achieved in designing well defined catalytic systems bearing aluminium[5], gallium[6], indium[7], lithium[8], magnesium[9], calcium[10], iron[11], zinc[12], lanthanides[13] and group 4 metals[14] as well as metal free catalysts like *N*-heterocyclic carbenes[15] to initiate the ROP of lactides. Despite the advances, the quest to synthesize new catalytic systems that can produce well defined polymer architecture is still a persisting interest among the researchers. We were interested in investigating catalytic systems based on group 5 metals for this purpose as these transition metals have not been explored much for the ROP of lactides. The first example of tantalum complexes containing the [tris(2-oxy-3,5-dimethylbenzyl)amine] ligand framework as catalysts for the ROP of lactides was reported by Verkade *et al*.[16] in 2002. Henceforth, only three other systems bearing niobium and tantalum metals as catalysts for the ROP of cyclic esters have been reported so far. In 2012, Antiñolo *et al*.[17] reported well controlled polymerization of lactones with medium to broad MWDs using hydridoniobocene complexes as catalysts. In 2013, we explored the catalytic acivities of imino phenoxide complexes of group 5 metals towards the ROP of lactides and cyclic esters.[18] Very recently, Redshaw *et al*.[19] have screened tetraphenolate niobium and tantalum complexes for the ROP of ε-caprolactone and the catalysts were proved to be efficient in terms of control and number average molecular weight (M_n). We have recently reported zwitterionic group 4 metal complexes containing aminophenol ligands for lactide polymerization and these catalysts were found to be stereoselective towards the polymerization and

[a] *Department of Chemistry, Indian Institute of Technology Patna, Patna- 800 013, Bihar, India.*
[b] *Department of Chemistry, Indian Institute of Technology Madras, Chennai- 600 036, Tamil Nadu, India. Fax: +91 44 22574202; Tel: +91 44 22574223; E-mail: dchakraborty@iitm.ac.in, debashis.iitp@gmail.com*

† Electronic Supplementary Information (ESI) available: Crystallographic data for the structural analysis of complex **2a** has been deposited at the Cambridge Crystallographic Data Center (CCDC). CCDC 1406201. See DOI: 10.1039/x0xx00000x

View Article Online
DOI: 10.1039/C6RA09789H

produced well controlled polymers with good M_n and MWDs.[20] Inspired by these results, we report here the synthesis, characterization and polymerization activities of niobium and tantalum complexes bearing aminophenol ligands.

Results and Discussion

Synthesis and characterization

The synthetic route for the preparation of niobium and tantalum complexes containing aminophenol ligands is shown in Scheme 1. The aminophenol ligands **L1**-**L3** were synthesized according to the standard literature procedure.[21] The reactions of Nb or Ta chlorides with the aminophenol ligands in 1:1 ratio at room temperature afforded orange/yellow coloured zwitterionic complexes **1**-**6** in good yield. Complexes **2** and **6** were crystallized from a solution of chloroform and ethanol as ethoxy substituted complexes **2a** and **6a**. Due to the presence of ethanol, two out of five chlorine atoms attached to the metal center were replaced by ethoxy groups in each case. This is similar to our observations with group 4 metals.[14f] All the complexes were dried and characterized by ^{1}H, ^{13}C NMR, ESI-MS and elemental analysis. From the ^{1}H NMR spectra, it was evident that two magnetically distinct -CH_2NCH_2 methylene hydrogens in **1**-**6** have their own resonances due to the diastereotopic character of the methylene hydrogens. The absence of the O-H signals of the ligands **L1**-**L3** (δ ~ 11-12 ppm respectively) in the ^{1}H NMR spectra of the metal complexes confirms the formation of **1**-**6** (Scheme 1).

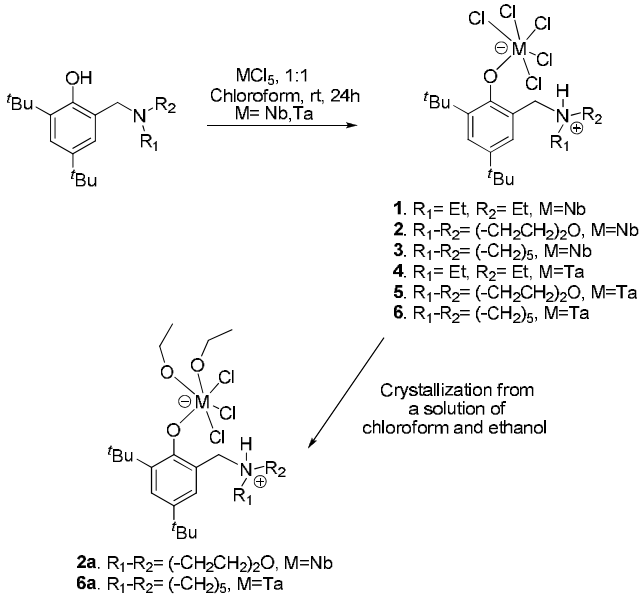

1. R_1= Et, R_2= Et, M=Nb
2. R_1-R_2= (-CH_2CH_2)$_2$O, M=Nb
3. R_1-R_2= (-CH_2)$_5$, M=Nb
4. R_1= Et, R_2= Et, M=Ta
5. R_1-R_2= (-CH_2CH_2)$_2$O, M=Ta
6. R_1-R_2= (-CH_2)$_5$, M=Ta

2a. R_1-R_2= (-CH_2CH_2)$_2$O, M=Nb
6a. R_1-R_2= (-CH_2)$_5$, M=Ta

Scheme 1. Synthesis of aminophenolate based niobium and tantalum complexes

A new signal, observed in the region δ 8.6-9.5 ppm, was identified as the peak corresponding to the protonated nitrogen atom. Based on our previous observations with group 4 chlorides, this protonation can be explained in terms of the basic character of the nitrogen atom in the aminophenolate complex.[20] The higher basic character of the sp^3 hybridised N atom of the aminophenol ligand resulted in the abstraction of proton from the generated side product of the reaction *i.e*. HCl and this positive charge was neutralised by a negative charge on the metal atom. The zwitterionic nature of the complexes was further confirmed by the single crystal X-ray diffraction studies. The protonation increased the electron withdrawing character of the nitrogen atoms. As a result of the presence of NH^+ moiety, the singlet –CH_2 peaks in ^{1}H and the corresponding peaks in ^{13}C NMR spectra of the metal complexes were deshielded compared to the aminophenol ligands. The expected molecular ion peaks of **1**-**6** were fragmented in the ESI-MS analyses and the observed base peaks were identified as peaks corresponding to the aminophenoxide ligands. Interestingly, in case of Nb complexes, the neutral aminophenoxide ligands dimerized to give peaks in higher *m/z* region. In contrast to the Nb complexes, the characteristic isotopic peaks at M+2 attribute to the presence of chlorine atoms in the molecular ions of Ta complexes. It clearly describes that in case of Ta complexes, the molecular ions correspond to the substituted metal complexes ($[L_2TaCl_4]^+$ where one chlorine atom bound to the metal center got replaced by a ligand fragment.

Single crystal X-ray diffraction studies

Single crystals of **2a**, suitable for X-ray diffraction studies, were obtained upon crystallization from a solution of chloroform and ethanol over a period of 2 weeks. Data collection for **6a** was attempted several times using different methods and techniques but failed due to its exceptional air sensitivity and significant decomposition during the period of data collection. The molecular structure of **2a** with selected bond lengths and bond angles are illustrated in Fig. 1. Complex **2a** crystallized from orthorhombic space group *Pna*2$_1$ space group. The geometry of the metal center in **2a** can be described as distorted octahedral where the axial positions are occupied by the aminophenolate ligand and one chlorine atom and the equatorial positions by the other two chlorine atoms and the oxygen atoms of the ethoxy groups. The selected bond lengths and bond angles are in good agreement with the literature reports of distorted octahedral complexes.[22] It can be observed from the solid state structures that the nitrogen atom of the amine sidearm is protonated and this positive charge is neutralised by a negative charge on the hexacoordinated metal center. The characteristic NH^+ peaks (δ 8.6-9.5 ppm) in the ^{1}H NMR spectra of the complexes support the protonation of the nitrogen atoms in the molecular structures. The zwitterionic complexes are stabilised by short range moderate electrostatic hydrogen bonding interactions.[23] The short distance between the nitrogen atom and one equatorial chlorine atom in **2a** is 3.1 Å which confirm the presence of hydrogen bonding interactions in the complex. The summary of crystal data refinement is given in Table 1.

Ring opening polymerization of *rac*-LA and *L*-LA

The catalytic potentials of **1**-**6** towards the ROP of lactides were systematically explored. A 200:1 monomer to catalyst

View Article Online
DOI: 10.1039/C6RA09789H

ratio was employed for the initial screening of the catalysts under solvent free condition. All the polymerizations were performed at 140 °C. The polymerization results, depicted in Table 2 and 3, suggest that all the catalysts behaved as moderately good initiators for the ROP of lactides although good degree of control over the polymerization parameters were achieved. All the polymers have number average molecular weights (M_n) close to the theoretical values and the molecular weight distributions (MWDs) are narrow.

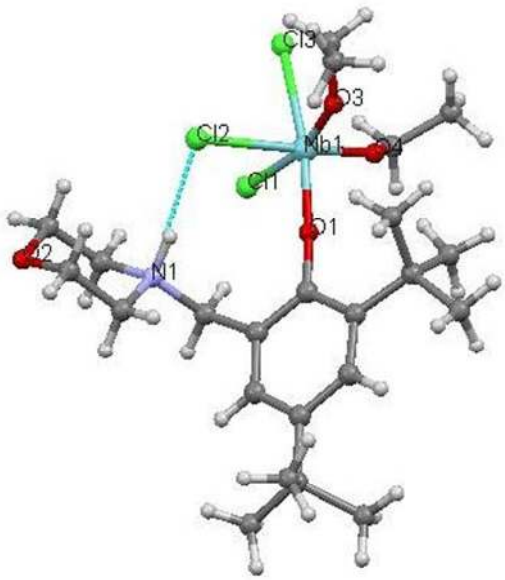

Fig. 1. Molecular structure of **2a**, Selected bond lengths (in Å) and bond angles (in °) are: O1-Nb1 1.92(4), Cl1-Nb1 2.44(2), Cl2-Nb1 2.51(2), Cl3-Nb1 2.46(2), O3-Nb1 1.85(5), O4-Nb1 1.85(2), O1-Nb1-Cl3 172.0(1), Cl1-Nb1-Cl2 85.7(6), O3-Nb1-O4 103.2(7), Cl1-Nb1-O4 84.0(7).

The homonuclear decoupled ^{1}H NMR spectrum indicates a heterotactic enrichment in the PLA produced from *rac*-LA with predominant *rmr* and *mrm* tetrads compared to *rmm*/*mmr* or *mmm* tetrads (Fig. S19, see ESI). The representative polymerizations at various monomer to catalyst concentrations were performed under neat condition. As can be seen from the plot of M_n and MWDs with $[M]_0/[Cat]_0$, the linear variations of M_n with the increasing ratios and almost invariable MWDs demonstrate the controlled nature of the polymerizations (Fig. 2). The observed turn over frequencies and molecular weights are in good line with the previous reports on group 5 complexes in the literature.[17-19] The plot of M_n vs % conversion represents an increase in M_n with the increment of the conversion of the lactide monomer (Fig. 3). The % conversion over time was monitored and the sigmoidal plot indicates an initial high rate of polymerization which reaches a stagnant value over time (Fig. S20, see ESI).

Table 1. Crystal data for the structure **2a**

Compound	2a
Molecular formula	$C_{23}H_{41}Cl_3NNbO_4$
Formula weight	594.83
T/K	298(2) K
Wavelength (Å)	0.71073
Crystal system,	Orthorhombic,
Space group	*Pna*2$_1$
a/Å	18.0256(14)
b/Å	15.4212(11)
c/Å	10.3922(6)
α (°)	90
β (°)	90
γ (°)	90
V/Å^3	2888.8(3)
Z, Calculated density(Mg/ m^3)	4, 1.368
Absorption coefficient (mm^{-1})	0.721
Reflections collected/Independent reflections	10273 / 3754
Data/restraints/parameters	3754 / 163 / 356
Goodness of fit on F^2	1.031
Final R indices [I >2σ(I)]	R_1 = 0.0334, wR_2 = 0.0737
R indices (all data)	R_1 = 0.0412, wR_2 = 0.0778

$R_1 = \sum||F_0| - |F_c||/\sum|F_0|$, $wR_2 = [\sum (F_0^2 - F_c^2)^2/\sum w(F_0^2)^2]^{1/2}$

The niobium complexes showed better activities compared to the tantalum complexes in terms of the time of the polymerizations. This is possibly due to the higher Lewis acidic character of niobium compared to tantalum which results in easier approach and coordination of the monomer to the metal center. The higher Lewis acidic character of the metal center plays an important role in the activity of the complexes and gives an insight into the observed higher activity of the chloride complexes **1**-**6** compared to the ethoxy substituted complexes **2a** and **6a**. The combined electronegativity from 5 chlorine atoms in **2** and **6** enhances the Lewis acidity of the metal center, while in case of ethoxy substituted complexes **2a** and **6a**, the electronegativity effect is obviously lesser because of the presence of 3 chlorine atoms around the metal center. Hence, the Lewis acidity of the metal center as well as the rate of polymerization is less in case of **2a** and **6a** compared to **2** and **6**. The observed variation in the time of polymerization with the change in the amine sidearm can only be reasonably explained in terms of the *s* character or the electronegativity of the nitrogen atom in the amine sidearm. As we move from the complexes having diethylamine sidearm to piperdine sidearm, the decrease in electronegativity of nitrogen results in decrease in the Lewis acidity of the metal center. Furthermore, we performed the polymerizations in presence of benzyl alcohol (BnOH) to probe the trend in activities. The activities of the catalysts increased in presence of BnOH and the polymerizations proceeded in a better controlled fashion with higher conversions achieved. The number average molecular weights (M_n) were closer to the theoretical values in presence of BnOH and MWDs were much narrower compared to the results observed under neat condition (Table 4).

View Article Online
DOI: 10.1039/C6RA09789H

Table 2. Polymerization data for *rac*-LA and *L*-LA catalyzed by complexes **1-6a** in 200:1 ratio at 140 °C

Entry	Cat.	LA	$[LA]_0/[Cat]_0$	time [a] (h)	Yield (%)	M_n(GPC) [b] (kg/mol)	$M_n^{(theoretical)}$ [c] (kg/mol)	TOF [d] (h^{-1})	M_w/M_n	P_r [e]
1	**1**	*rac*-LA	200/1	10	96	26.28	29.12	19.40	1.18	0.67
2	**2**	*rac*-LA	200/1	13	95	26.47	29.13	14.77	1.19	0.66
3	**2a**	*rac*-LA	200/1	20	96	28.50	29.13	9.80	1.16	0.68
4	**3**	*rac*-LA	200/1	14	94	27.11	29.13	13.71	1.17	0.67
5	**4**	*rac*-LA	200/1	14	94	26.48	29.12	13.57	1.20	0.69
6	**5**	*rac*-LA	200/1	17	96	27.30	29.13	11.29	1.19	0.69
7	**6**	*rac*-LA	200/1	18	93	28.12	29.13	10.67	1.20	0.67
8	**6a**	*rac*-LA	200/1	22	96	29.17	29.13	8.82	1.18	0.68
9	**1**	*L*-LA	200/1	9	95	25.54	29.12	21.56	1.17	
10	**2**	*L*-LA	200/1	10	94	25.15	29.13	19.60	1.15	
11	**2a**	*L*-LA	200/1	18	95	27.97	29.13	10.89	1.15	
12	**3**	*L*-LA	200/1	12	93	25.60	29.13	16.17	1.17	
13	**4**	*L*-LA	200/1	13	92	26.02	29.12	14.77	1.18	
14	**5**	*L*-LA	200/1	18	96	26.44	29.13	10.78	1.18	
15	**6**	*L*-LA	200/1	18	95	27.27	29.13	10.89	1.20	
16	**6a**	*L*-LA	200/1	21	96	28.69	29.13	9.24	1.19	

[a]Time of polymerization was measured by quenching the polymerization reaction when all the monomer were found to be consumed. [b]Measured by GPC at 27 ℃ in THF relative to polystyrene standards and corrected using the Mark-Houwink factor of 0.58 for M_n. [24 c]$M_n^{(theoretical)}$ at 100% = $[M]_0/[C]_0$ × molecular weight of monomer + molecular weight of end group. [d]TOFs were calculated as (mol of LA consumed) / (mol of catalyst × time of polymerization). [e]The probability for heterotactic enchainment was calculated from homonuclear decoupled ^{1}H NMR spectrum.

Table 3. Polymerization data for *rac*-LA catalyzed by complexes **2**, **2a**, **6** and **6a** in different $[rac\text{-LA}]_0/[Cat]_0$ ratios at 140 °C

Entry	Cat.	$[rac\text{-LA}]_0/[Cat]_0$	time [a] (h)	Yield (%)	M_n(GPC) [b] (kg/mol)	$M_n^{(theoretical)}$ [c] (kg/mol)	TOF [d] (h^{-1})	M_w/M_n	P_r [e]
1	**2**	200/1	13	95	26.28	29.12	19.40	1.18	0.66
2	**2**	400/1	25	96	54.38	57.94	15.52	1.19	
3	**2**	800/1	48	95	111.93	115.60	16.17	1.21	
4	**2a**	200/1	20	96	28.50	29.13	9.80	1.16	0.68
5	**2a**	400/1	37	97	55.24	57.96	10.59	1.17	
6	**2a**	800/1	65	97	112.40	115.61	12.06	1.17	
7	**6**	200/1	18	93	28.12	29.12	10.67	1.20	0.67
8	**6**	400/1	34	95	51.59	57.94	11.17	1.19	
9	**6**	800/1	57	94	112.39	115.60	13.47	1.22	
10	**6a**	200/1	22	96	27.61	29.13	8.82	1.18	0.68
11	**6a**	400/1	39	94	56.19	57.96	9.74	1.17	
12	**6a**	800/1	67	94	113.68	115.61	11.46	1.21	

[a]Time of polymerization was measured by quenching the polymerization reaction when all the monomer were found to be consumed. [b]Measured by GPC at 27 ℃ in THF relative to polystyrene standards and corrected using the Mark-Houwink factor of 0.58 for M_n. [24 c]$M_n^{(theoretical)}$ at 100% = $[M]_0/[C]_0$ × molecular weight of monomer + molecular weight of end group. [d]TOFs were calculated as (mol of LA consumed) / (mol of catalyst × time of polymerization). [e]The probability for heterotactic enchainment was calculated from homonuclear decoupled ^{1}H NMR spectrum.

View Article Online
DOI: 10.1039/C6RA09789H

Table 4. Polymerization data of *rac*-LA in presence of BnOH catalyzed by complexes **1**-**6a** in 200:1:5 ratio at 140 °C

Entry	Cat.	$[LA]_0/[Cat]_0/[BnOH]_0$	LA	time [a] (h)	Yield (%)	M_n(GPC)[b] (kg/mol)	$M_n^{(theoretical)}$[c] (kg/mol)	M_w/M_n	P_r[d]
1	**1**	200/1/5	*rac*-LA	6	97	4.67	5.87	1.11	0.69
2	**2**	200/1/5	*rac*-LA	8	98	4.93	5.87	1.09	0.70
3	**2a**	200/1/5	*rac*-LA	15	98	5.10	5.87	1.10	0.71
4	**3**	200/1/5	*rac*-LA	8	97	4.95	5.87	1.12	0.70
5	**4**	200/1/5	*rac*-LA	9	96	4.88	5.87	1.08	0.72
6	**5**	200/1/5	*rac*-LA	14	98	5.01	5.87	1.10	0.68
7	**6**	200/1/5	*rac*-LA	16	97	5.23	5.87	1.11	0.67
8	**6a**	200/1/5	*rac*-LA	18	96	5.15	5.87	1.13	0.71
9	**1**	200/1/5	*L*-LA	5	96	4.59	5.87	1.11	
10	**2a**	200/1/5	*L*-LA	15	97	4.81	5.87	1.12	
11	**3**	200/1/5	*L*-LA	8	98	4.77	5.87	1.10	
12	**4**	200/1/5	*L*-LA	10	96	5.12	5.87	1.14	
13	**5**	200/1/5	*L*-LA	14	96	4.92	5.87	1.11	
14	**6a**	200/1/5	*L*-LA	16	97	4.85	5.87	1.12	

[a]Time of polymerization was measured by quenching the polymerization reaction when all the monomer were found to be consumed. [b]Measured by GPC at 27 °C in THF relative to polystyrene standards and corrected using the Mark-Houwink factor of 0.58 for M_n.[24] [c]$M_n^{(theoretical)}$ at 100% = $[M]_0/[C]_0$ × molecular weight of monomer + molecular weight of end group. [d]The probability for heterotactic enchainment was calculated from homonuclear decoupled ^{1}H NMR spectrum.

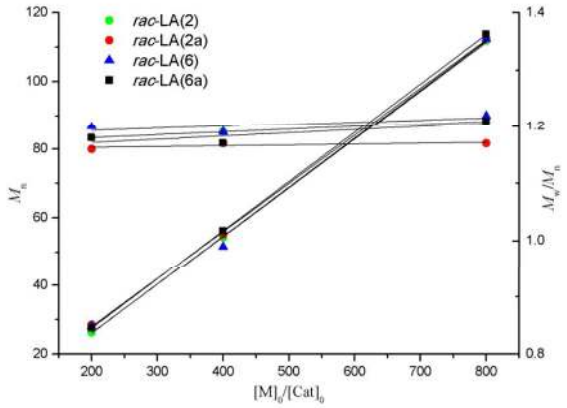

Fig. 2. Plot of M_n and MWD *vs.* $[M]_0/[Cat]_0$ for *rac*-LA polymerization at 140 °C using **2**, **2a**, **6** and **6a**

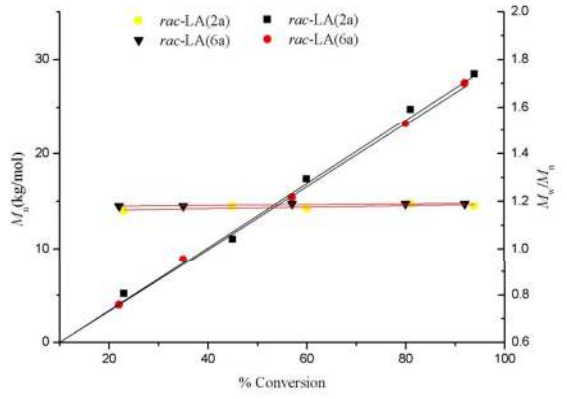

Fig. 3. Plot of M_n and M_w/M_n *vs.* % conversion for *L*-LA and *rac*-LA polymerization at 140 °C using **2a** and **6a**

In the next segment of our study, we performed the kinetics for the polymerization of rac-LA using **2a** and **6a** in the ratio $[rac\text{-LA}]_0/[Cat]_0$ = 200 at 140 °C. From the plot it was ascertained that there is a first-order dependence of the rate of polymerization on the monomer concentration without any induction period (Fig. 4). The plot of $\ln[rac\text{-LA}]_0/[rac\text{-LA}]_t$ vs. time was found to be linear. The values of the apparent rate constants (k_{app}) were evaluated from the slopes of these lines and were found to be 0.121 h^{-1} and 0.101 h^{-1} for **2a** and **6a** repectively.

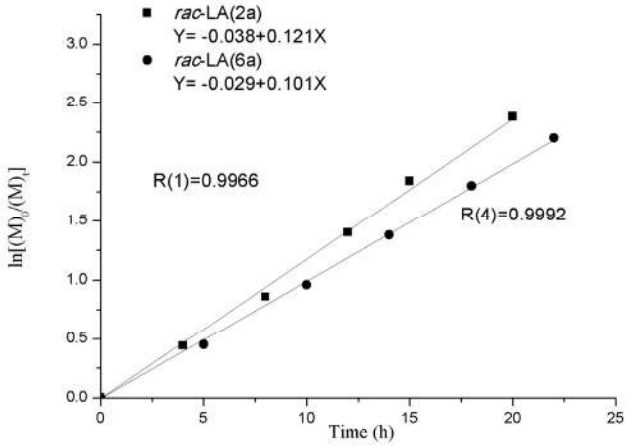

Fig. 4. Semi-logarithmic plots of *rac*-LA, conversion initiated by **2a** and **6a** over time

Low molecular weight oligomers were prepared by stirring *rac*-LA and catalyst **2a** in 10:1 ratio at 140 °C in order to explore the polymerization mechanism. The resultant crude product was dissolved in minimum volume of CH_2Cl_2 and poured subsequently into cold methanol to precipitate the oligomers.

View Article Online
DOI: 10.1039/C6RA09789H

The analyses of the ^{1}H NMR and MALDI-TOF mass spectra suggest that the oligomer contains aminophenol ligand as the end terminal group (Fig. 5 and 6). All the major peaks in the MALDI-TOF mass spectrum, equally spaced by 72 a.m.u., are present as acetonitrile (CH_3CN) adducts (Fig. 6). The intensities of the minor peaks are maginal. The peaks with small intensities at the immediate left of the major peaks were identified as Na adducts. The absence of the O-H signal in the ^{1}H NMR spectrum of the oligomer ensures that the free ligand is not present in the crude product and suggests that the ring opening polymerization was initiated by the ligand through the M-O linkage. The ethoxy group is a mere spectator during the ROP and does not initiate the polymerization although it had influence on the Lewis acidic character of the metal center. we also tested blank polymerization tests in presence of free ligands and no polymeric product was formed in that case which signifies the importance of the Lewis acidic metal center for the coordination of the lactide monomer to the catalyst. The probable mechanism can be inferred from the literature reports as follows. After the precursor formation, the lactide monomer inserts into the M-O bond which is initiated by the nucleophilic attack of the ligand on the carbonyl carbon of the monomer. This is followed by the cleavage of the acyl-oxygen bond which results in the opening of the ring (Scheme 2).[1b,25]

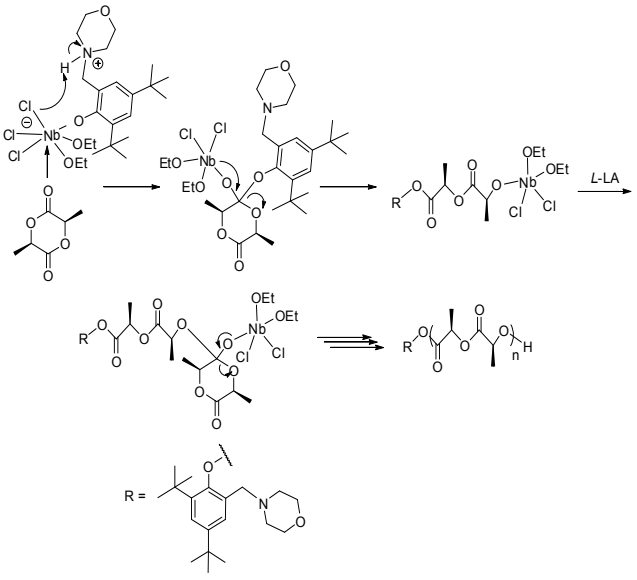

Scheme 2. Proposed mechanism for the polymerization of lactide using **2a**

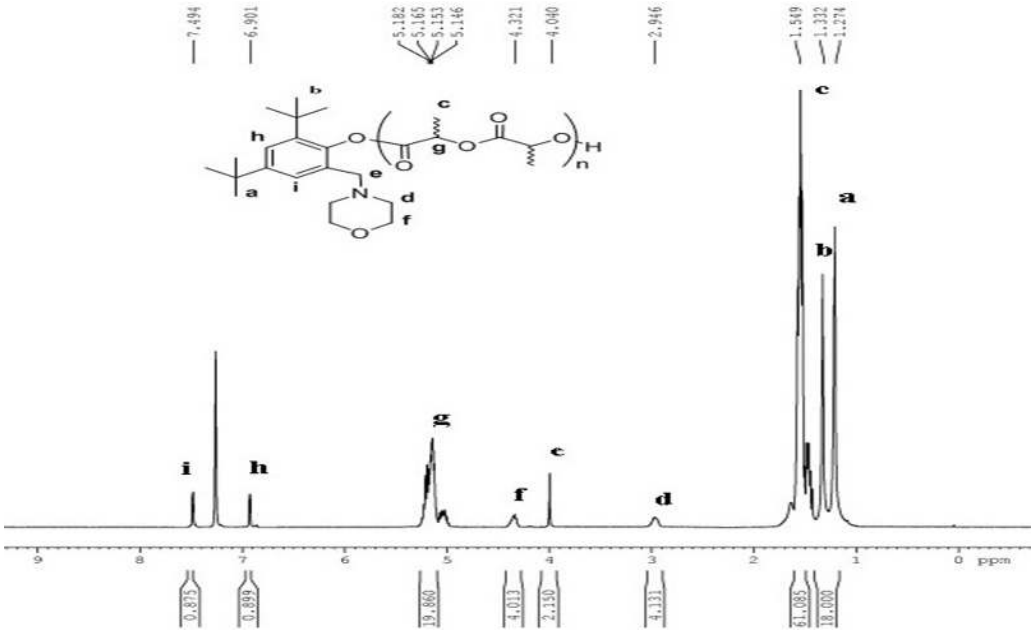

Fig. 5. ^{1}H NMR spectrum (500 MHz, $CDCl_3$) of the crude product obtained from a reaction between *rac*-LA and **2a** in 10:1 ratio at 140 °C.

View Article Online
DOI: 10.1039/C6RA09789H

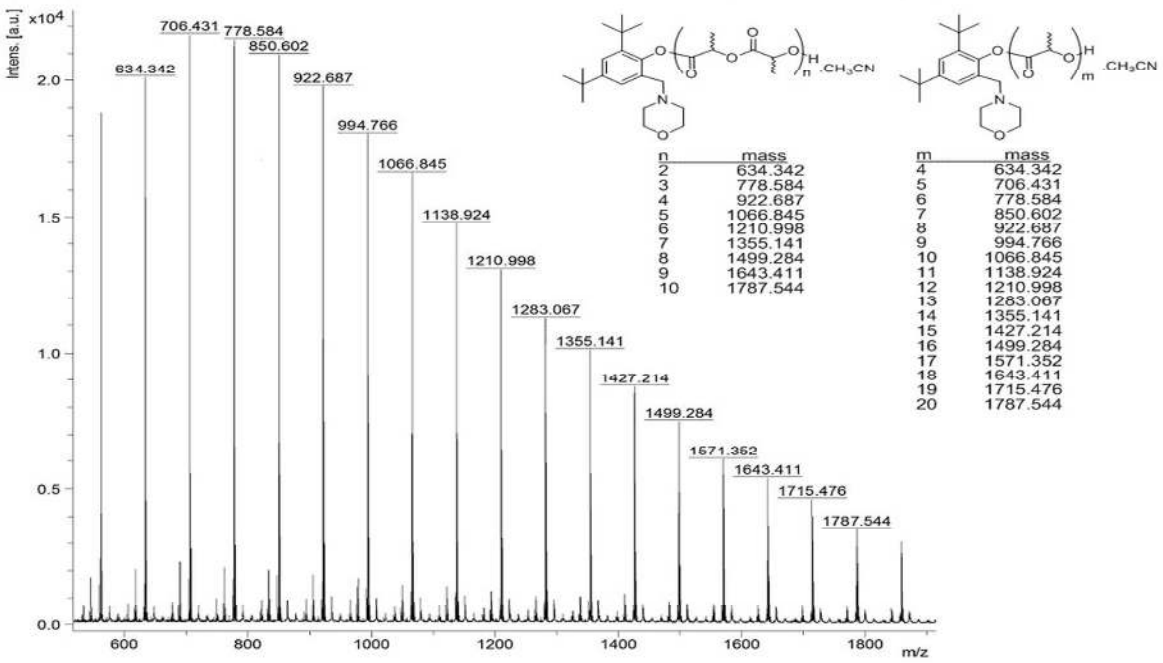

Fig. 6. MALDI-TOF spectrum of the crude product obtained from a reaction between *rac*-LA and **2a** in 10:1 ratio at 140 °C

Low molecular weight oligomers were synthesized from a reaction between *rac*-LA and **2a** in presence of BnOH in 20:1:5 ratio and subjected to ^{1}H NMR and MALDI-TOF MS analyses in order to know about the end group of the polymer produced in presence of BnOH (Fig. S21 and S22, see Supplementary Information). A series of peaks were observed in the MALDI-TOF MS spectrum at a regular interval of 72 a.m.u and were identified as proton adducts of the benzyloxy capped linear PLA. From the ^{1}H NMR spectrum of the oligomer, it is clear that the PLA is end capped with a –OBn group as the peaks corresponding to the ligands were absent. The higher catalytic activities of the complexes in presence of BnOH was due to the formation of more active benzyloxy substituted metal complex prior to the polymerization and this –OBn group further inititated the polymerization.[26]

Computational studies

The density functional theory calculations were carried out on **2**, **6**, **2a** and **6a** in order to understand the reactivity or stability of the complexes. All the complexes were first optimized at B3LYP/LANL2DZ level. The frontier molecular orbital analysis of the optimized geometries illustrates a vivid approach towards the reactivity of the complexes. Based on Koopman's theorem for closed shell molecules, Pearson defined a relation between the chemical hardness (η) and reactivity of a species as η = 1/2(I-A), where I and A represents the ionization potential and electron affinity respectively. The ionization potential can be directly related to the energy of the highest occupied molecular orbital ($-\varepsilon_{HOMO}$), whereas the energy of the lowest unoccupied molecular orbital ($-\varepsilon_{LUMO}$) depicts the electron affinity. Hence, the HOMO-LUMO energy gap is an important parameter in understanding the chemical stability of a complex. As the energy gap between HOMO and LUMO increases, the hardness or stability also increases leading to a decrease in the polarizability or reactivity.[27]

View Article Online
DOI: 10.1039/C6RA09789H

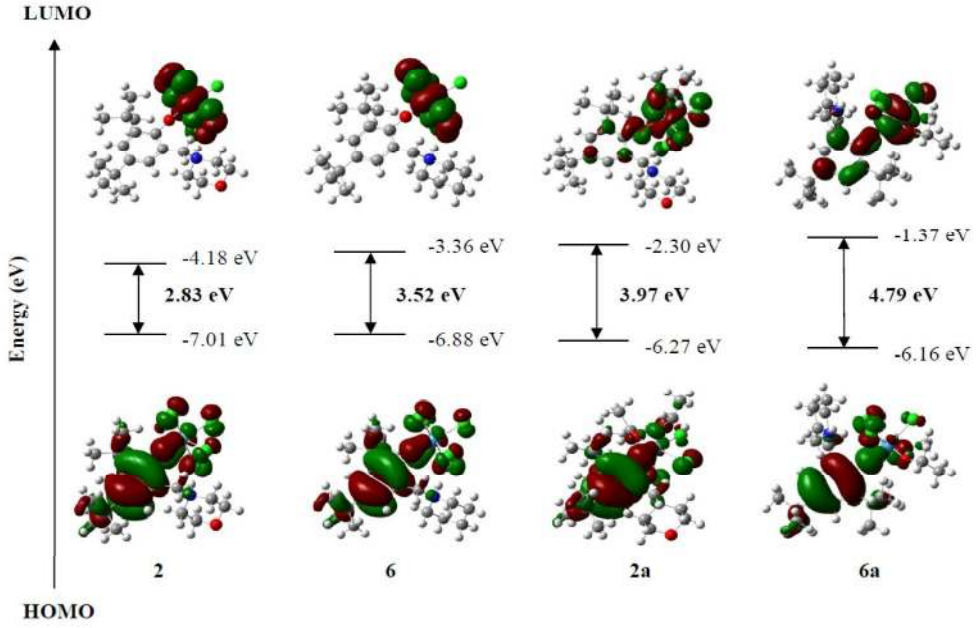

Fig. 7. The difference in energy between HOMO and LUMO for **2**, **2a**, **6** and **6a**.

We utilized the same approach in explaining the reactivity in our study. In general, the HOMO-LUMO energy gaps of the Nb complexes (2.83 eV and 3.97 eV for **2** and **2a**) are significantly lower than that of Ta complexes (3.52 eV and 4.79 eV for **6** and **6a**) which indicate towards higher reactivity of the Nb complexes (**2** and **2a**) compared to the Ta complexes (**6** and **6a**) (Fig. 7). Interestingly, ethoxy substituted complexes **2a** and **6a** (where two out of the five chlorine atoms bonded to the metal center were substituted by ethoxy groups during crystallization) possess higher HOMO-LUMO energy gap compared to the unsubstituted pentachloro analogues. The higher reactivity of **2** and **6** compared to **2a** and **6a** towards the ROP of lactides corroborates this theoretical result.

Mulliken population analyses of these complexes revealed that the ROP was initiated by the phenolic ligand through the M-O linkage. In case of **2a** and **6a**, the phenolic O atoms bear higher negative charges (-0.624 and -0.632 for **2a** and **6a** respectively) compared to the ethoxy O atoms (-0.523 and -0.539 for **2a** and **6a** respectively) which confirm that the ethoxy group act as a mere spectator during the initiation. Molecular Electrostatic Potential (MEP) mapped surface, which displays the variation in the electrostatic potential of different regions of a molecule, is a good guide for assessing the most probable site for electrophilic attack in the molecule. The increase in potential is represented by a change from blue to red color. The MEP plots of **2a** and **6a** are in good agreement with the Mulliken population analyses wherein the phenolic O atoms belong to the more negatively charged yellow colored region compared to the ethoxy O atoms (Fig. 8 and Fig. S23, see ESI).

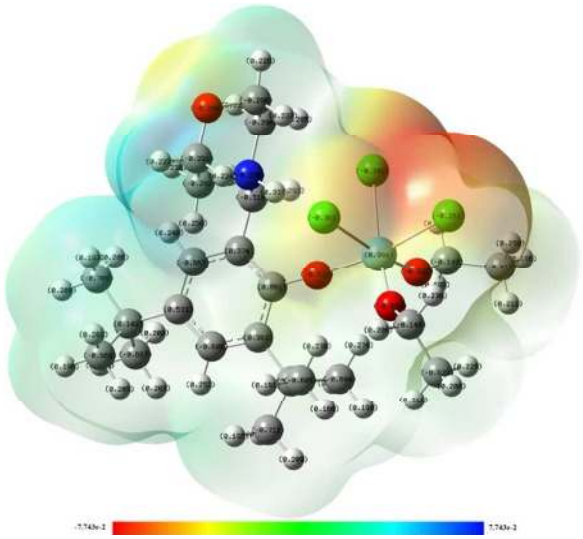

Fig. 8. The MEP mapped surface of **2a** calculated at an isovalue of 0.004 representing electrostatic potential.

Conclusion

In summary, a series of niobium and tantalum complexes containing aminophenol ligands were synthesized and fully characterized by ^{1}H, ^{13}C NMR, ESI-MS spectroscopy and elemental analyses. Suitable crystals for single crystal X-ray diffraction study could be grown from a solution of chloroform

View Article Online
DOI: 10.1039/C6RA09789H

and ethanol only after several attempts from other solvents. Complex **2** crystallized as ethoxy substituted complex **2a** upon attempting crystallization from the solvent mixture of chloroform and ethanol. The molecular structure showed that the complex possessed a similar zwitterionic character as observed for our earlier reports on group 4 metals bearing aminophenol ligands. The zwitterionic complexes are stabilised by moderate electrostatic hydrogen bonding interaction between the NH^+ moiety and the chlorine atom. All the compounds were proved to be active towards the ROP of lactides and afforded PLA with good number average molecular weight (M_n) and narrow molecular weight distributions (MWDs). Although our earlier reports of group 4 complexes containing similar ligands were more efficient in terms of control over polymerization, the niobium and tantalum complexes afforded better results compared to the few reports on group 5 complexes in the literature.[17,19] Microstructural analyses revealed that all the complexes produced heterotactic enriched PLAs. The MALDI-TOF and ^{1}H NMR spectra proved tha the ligand initiates the polymerization under solvent free condition.

Experimental

Materials and general details

All the experiments were performed under purified argon atmosphere using either standard schlenk technique or in a glove box. The solvents were freshly distilled from suitable drying agent (chloroform over calcium hydride and ethanol over activated 10% m/v of 3 Å molecular sieves for 5 days followed by heating over iodine-activated magnesium[28]) and degassed prior to use. *rac*-LA, *L*-LA, $CDCl_3$ for NMR studies were purchased from Aldrich and. *rac*-LA and *L*-LA were sublimed under vacuum twice whereas $CDCl_3$ was purified by drying over calcium hydride followed by distillation prior to use. All chemicals needed for the synthesis of the ligands, $NbCl_5$ and $TaCl_5$ were purchased from Aldrich and used as such without any further purification. The ligands **L1**-**L3** were prepared according to the standard literature procedures[21] and purified by azeotropic distillation before storing in the glove box. All ^{1}H and ^{13}C NMR spectra were recorded on 400 MHz Bruker Avance or 500 MHz Bruker Ascend instrument with chemical shifts given in parts per million (ppm). ESI-MS spectra of the compounds were performed using Waters Q-TOF micro mass spectrometer. Elemental analyses were performed using Perkin Elmer Series 11 analyzer. The MALDI-TOF of oligomers werr performed on a Bruker Daltonics instrument using dihydroxybenzoic acid matrix. Molecular weights and MWDs of the polymer samples obtained by the ring opening polymerization of lactide monomers were determined by using a GPC instrument with Waters 510 pump and Waters 410 differential refractometer as the detector. Three columns namely WATERS STRYGEL-HR5, STRYGEL-HR4 and STRYGEL-HR3 each of dimensions (7.8×300 mm) were connected in series. Measurements were done in THF at 27 °C. The number average molecular weights (M_n) and molecular weight distributions (M_w/M_n) (MWDs) of polymers were measured relative to polystyrene standards.

Synthesis of 1-9

The general procedure for the synthesis of **1**-**6** is given below. The aminophenol ligand **L1** or **L2** or **L3** (0.10 mmol) was dissolved in 10 mL of dry chloroform and was added to the solution of $NbCl_5$ or $TaCl_5$ (0.10 mmol) in 5 mL of chloroform in 1:1 ratio at -24 °C in an argon filled glove box. The colour of the reaction mixture immediately changed to orange in case of Nb complexes and yellow in case of Ta complexes. The reaction mixture was stirred and allowed to come to room temperature. After 24 hours of vigorous stirring, the solvent was removed under vacuum to give complexes **1**-**6**.

Complex 1. (Yield 48 mg, 86%). ^{1}H NMR (400 MHz, $CDCl_3$, ppm): δ = 1.33 (s, 9H, -C(CH_3)$_3$), 1.38 (m, 6H, -CH_2CH_3), 1.63 (s, 9H, -C(CH_3)$_3$), 3.15 (m, 2H, -C(*H*)HCH_3), 3.46 (m, 2H, -C(H)*H*CH_3), 4.43 (s, 2H, Ar-CH_2), 7.02 (m, 1H, Ar-*H*), 7.56 (m, 1H, Ar-*H*), 8.86 (s, 1H, N*H*-CH_2). ^{13}C NMR (100 MHz, $CDCl_3$, ppm): δ = 16.7, 30.2, 31.9, 33.3, 34.1, 50.1, 61.2, 123.0, 126.0, 126.9, 137.1, 140.1 157.2. ESI *m/z* calculated for $[M]^+$. $C_{38}H_{64}N_2O_2$: 580.93, found 581.55. Anal. Calc. for $C_{19}H_{33}Cl_5NNbO$: C, 40.63; H, 5.92; N, 2.49; found C, 41.04; H, 5.88; N, 2.56.

Complex 2. (Yield 53 mg, 89%). The resultant orange solid was crystallized from a solution of chloroform and ethanol. Due to the presence of ethanol, complex **2** crystallized as an ethoxy substituted complex **2a**. ^{1}H NMR (400 MHz, $CDCl_3$, ppm): δ = 1.27 (s, 9H, -C(CH_3)$_3$), 1.31 (m, 6H, -OCH_2CH_3), 1.47 (s, 9H, -C(CH_3)$_3$), 3.05 (m, 4H, -NCH_2CH_2), 3.99 (s, 2H, Ar-CH_2), 4.25 (m, 4H, -OCH_2CH_2), 4.92-4.97 (m, 6H, -OCH_2CH_3), 6.91-6.92 (m, 1H, Ar-*H*), 7.49-7.50 (m, 1H, Ar-*H*), 9.39 (s, 1H, N*H*-CH_2). ^{13}C NMR (100 MHz, $CDCl_3$, ppm): δ = 16.6, 31.3, 31.4, 34.3, 35.6, 52.1, 60.5, 63.8, 74.7, 127.2, 128.2, 129.0, 141.9, 144.1, 159.9. ESI *m/z* calculated for $[M+CH_3CN]^+$. $C_{40}H_{63}N_3O_4$: 648.89, found 647. Anal. Calc. for $C_{19}H_{31}Cl_5NNbO_2$: C, 39.64; H, 5.43; N, 2.43; found C, 40.15; H, 5.51; N, 2.46.

Complex 3. (Yield 51 mg, 88%). ^{1}H NMR (400 MHz, $CDCl_3$, ppm): δ = 1.33 (s, 9H, -C(CH_3)$_3$), 1.42 (m, 2H, -$CH_2CH_2CH_2$), 1.51 (s, 9H, -C(CH_3)$_3$), 1.59 (m, 4H, -$CH_2CH_2CH_2$), 3.00 (m, 4H, -NCH_2CH_2), 3.89 (s, 2H, Ar-CH_2), 6.99-6.70 (m, 1H, Ar-*H*), 7.51-7.52 (m, 1H, Ar-*H*), 8.81 (s, 1H, N*H*-CH_2). ^{13}C NMR (100 MHz, $CDCl_3$, ppm): δ = 22.4, 24.8, 33.0, 33.4, 36.2, 37.5, 54.9, 62.9, 128.1, 132.9, 133.5, 142.8, 145.6, 158.9. ESI *m/z* calculated for $[M+CH_3CN]^+$. $C_{42}H_{67}N_3O_2$: 644.95, found 643. Anal. Calc. for $C_{20}H_{33}Cl_5NNbO$: C, 41.87; H, 5.80; N, 2.44; found C, 42.11; H, 5.86; N, 2.50.

Complex 4. (Yield 59 mg, 91%). ^{1}H NMR (400 MHz, $CDCl_3$, ppm): δ = 1.29 (s, 9H, -C(CH_3)$_3$), 1.36 (m, 6H, -CH_2CH_3), 1.59 (s, 9H, -C(CH_3)$_3$), 3.13 (m, 2H, -C(*H*)HCH_3), 3.42 (m, 2H, -C(H)*H*CH_3), 4.42 (s, 2H, Ar-CH_2), 7.00 (m, 1H, Ar-*H*), 7.52 (m, 1H, Ar-*H*), 8.75 (s, 1H, N*H*-CH_2). ^{13}C NMR (100 MHz, $CDCl_3$, ppm): δ = 15.0, 27.2, 29.0, 32.1, 33.1, 48.9, 60.1, 121.8, 124.9, 125.4, 136.2, 138.3 156.1. ESI *m/z* calculated for $[M]^+$. $C_{38}H_{64}Cl_4N_2O_2Ta$: 903.69, found 903.06. Anal. Calc. for

View Article Online
DOI: 10.1039/C6RA09789H

$C_{19}H_{33}Cl_5NOTa$: C, 35.13; H, 5.12; N, 2.16; found C, 35.42; H, 5.29; N, 2.21.

Complex 5. (Yield 56 mg, 86%). ^{1}H NMR (400 MHz, $CDCl_3$, ppm): δ = 1.26 (s, 9H, -C(CH_3)$_3$), 1.39 (s, 9H, -C(CH_3)$_3$), 2.89 (m, 4H, -CH_2CH_3), 3.89 (s, 2H, Ar-CH_2), 4.10 (m, 4H, -OCH_2CH_2), 6.88-6.89 (m, 1H, Ar-*H*), 7.40-7.41 (m, 1H, Ar-*H*), 9.12 (s, 1H, N*H*-CH_2). ^{13}C NMR (100 MHz, $CDCl_3$, ppm): δ = 30.1, 30.2, 33.2, 35.1, 51.2, 60.0, 63.0, 127.1, 128.1, 129.6, 140.1, 144.1 160.5. ESI *m/z* calculated for $[M]^+$. $C_{38}H_{60}Cl_4N_2O_4Ta$: 931.65, found 931. Anal. Calc. for $C_{19}H_{31}Cl_5NO_2Ta$: C, 34.39; H, 4.71; N, 2.11; found C, 34.64; H, 4.88; N, 2.16.

Complex 6. (Yield 60 mg, 91%). The resultant yellow solid was crystallized from a solution of chloroform and ethanol. Due to the presence of ethanol, complex **6** crystallized as an ethoxy substituted complex **6a**. ^{1}H NMR (400 MHz, $CDCl_3$, ppm): δ = 1.27 (s, 9H, -C(CH_3)$_3$), 1.29 (m, 6H, -OCH_2CH_3), 1.40 (m, 2H, -$CH_2CH_2CH_2$), 1.51 (s, 9H, -C(CH_3)$_3$), 1.53 (m, 4H, -$CH_2CH_2CH_2$), 2.92-2.95 (m, 4H, -NCH_2CH_2), 3.89 (s, 2H, Ar-CH_2), 6.89-6.90 (m, 1H, Ar-*H*), 7.48-7.49 (m, 1H, Ar-*H*), 8.67 (s, 1H, N*H*-CH_2). ^{13}C NMR (100 MHz, $CDCl_3$, ppm): δ = 17.3, 22.1, 22.9, 31.2, 31.6, 34.4, 35.7, 53.2, 60.1, 127.1, 128.7, 129.2, 141.9, 143.8, 159.1. ESI *m/z* calculated for $[M]^+$. $C_{40}H_{64}Cl_4N_2O_2Ta$: 927.71, found 927. Anal. Calc. for $C_{20}H_{33}Cl_5NTaO$: C, 36.30; H, 5.03; N, 2.12; found C, 36.86; H, 5.14; N, 2.23.

X-ray crystallography

Suitable crystals for X-ray diffraction studies of **2a** were obtained by crystallization from a solution of chloroform and ethanol. Crystals of **2a** were obtained from this solvent mixture only after several attempts from other solvents. Single crystal of proper size was selected from mother liquor and mounted on Bruker AXS (Kappa Apex 2) CCD diffractometer equipped with graphite monochromated Mo (Kα) (λ = 0.7107 Å) radiation source. A full sphere of data was collected with 100% completeness for ϑ up to 25°. ω and φ scans were employed to collect the data. The frame width for ω was set to 0.5 for data collection. The frames were integrated and data were reduced to Lorentz and polarization corrections using SAINT-NT. The data set was subjected to multi-scan absorption. The structure was solved using SIR-92 and refined using SHELXL-97.[29] All non-H atoms were located from successive Fourier maps, and hydrogen atoms were refined using a riding model. Anisotropic thermal parameters were used for all non-H atoms, and fixed isotropic parameters were used for H atoms. These data were deposited with CCDC with the following CCDC numbers: 1406201 (**2a**).

General procedure for the polymerization of *rac*-LA and *L*-LA

The polymerizations were carried out under solvent free condition by rapidly stirring the monomer and the catalyst in a closed glass vessel to 140 °C till the time the melt had become viscous. 0.25 g of *rac*-LA or *L*-LA and 8.67 µmol of the catalyst were charged in 200:1 ratio in a dry glass vessel equipped with a magnetic stirrer bar. After the reaction time, the reaction mixture was dissolved in minimum volume of dichloromethane and then poured into cold methanol to precipitate the polymers. The resultant polymers were dried under vacuum to a constant weight. The conversion yield of *rac*-LA and *L*-LA were analyzed by ^{1}H NMR spectroscopic studies. The number average molecular weight (M_n) and M_w/M_n (MWDs) were determined by GPC measurements.

Studies of kinetics for the polymerization of lactides

The kinetic studies were performed by polymerizing *rac*-LA using **2a** or **6a** in 200:1 ratio at 140 °C. We carried out a set of five polymerizations for each catalyst. 0.035 mmol of **2a** or **6a** and 1 g of monomer were loaded in each sealed tube under argon atmosphere. The contents were stirred and immersed in a bath at 140 °C. The time of polymerization for maximum conversion of lactide monomer using each catalyst as determined earlier was divided into five regular intervals. Each of the set of five polymerizations was allowed to run for different assumed time interval. After that, the contents were quenched separately by dissolving in minimum amount of dichloromethane followed by pouring into cold methanol and analyzed by ^{1}H NMR. The $[rac\text{-LA}]_0/[rac\text{-LA}]_t$ ratio was evaluated by integrating the peaks corresponding to the methine proton for the monomer and polymer. Apparent rate constant (k_{app}) were calculated from the slopes of the best-fit lines.

Computational details

The molecular geometry optimizations were calculated using GAUSSIAN 09 (Rev C.01) package of quantum chemical programs.[30] The calculations were carried out using B3LYP method, a hybrid function comprising of Becke's three parameter functional (B3) and a mixture of HF with DFT exchange terms associated with the gradient corrected correlation functional of Lee, Yang and Parr (LYP) and LANL2DZ basis set.[31]

Acknowledgements

The authors are grateful to the Department of Science and Technology, New Delhi for funding this work. SKR thanks the University Grants Commission, New Delhi for a research fellowship.

References

1 (a) A. Sauer, A. Kapelski, C. Fliedel, S. Dagorne, M. Kol and J. Okuda, *Dalton Trans*., 2013, **42**, 9007-9023; (b) O. Dechy-Cabaret, B. Martin-Vaca and D. Bourissou, *Chem. Rev*., 2004, **104**, 6147-6176; (c) F. E. Kohn, J. G. V. Ommen and J. Feijen, *Eur. Polym. J.*, 1983, **19**, 1081-1088.

2 (a) Z. Zhong, P. J. Dijkstra and J. Feijen, *Angew. Chem. Int. Ed.*, 2002, **41**, 4510-4513; (b) Y. Ikada and H. Tsuji, *Macromol. Rapid Commun.*, 2000, **21**, 117-132; (c) C. T. Altaf, H. Wang, M. Keram, Y. Yang and H. Ma, *Polyhedron*, 2014, **81**, 11-20; (d) Y. Sun, L. Wang, D. Yu, N. Tang and J. Wu, *Journal of Molecular Catalysis A: Chemical*, 2014, **393**, 175-181.

View Article Online
DOI: 10.1039/C6RA09789H

3 (a) R. H. Platel, L. M. Hodgson and C. K. Williams, *Polym. Rev.*, 2008, **48**, 11–63; (b) A. Amgoune, C. M. Thomas, T. Roisnel and J.-F. Carpentier, *Chem. Eur. J.*, 2006, **12,** 169-179; (c) J. Wu, T.-L. Yu, C.-T. Chen and C.-C. Lin, *Coord. Chem. Rev.*, 2006, **250**, 602–626; (d) C. A. Wheaton, P. G. Hayes and B. J. Ireland, *Dalton Trans.*, 2009, 4832–4846; (e) N. E. Kamber, W. Jeong, R. M. Waymouth, R. C. Pratt, B. G. G. Lohmeijer and J. L. Hedrick, *Chem. Rev.*, 2007, **107**, 5813–5840; (f) J. Zhang, C. Jian, Y. Gao, L. Wang, N. Tang and J. Wu, *Inorg. Chem.*, 2012, **51**, 13380-13389; (g) A. Stopper, J. Okuda and M. Kol, *Macromolecules*, 2012, **45**, 698-704.

4 (a) M. J. Stanford and A. P. Dove, *Chem. Soc. Rev.*, 2010, **39**, 486-494; (b) C. M. Thomas, *Chem. Soc. Rev.*, 2010, **39**, 165-173; (c) P. J. Dijkstra, H. Du and J. Feijen, *Polym. Chem.* 2011, **2**, 520-527.

5 (a) N. Spassky, M. Wisniewski, C. Pluta and A. Le Borgne, *Macromol. Chem. Phys.* 197 (1996) 2627; (b) P. Hormnirun, E. L. Marshall, V. C. Gibson, A. J. P. White and D. J. Williams, *J. Am. Chem. Soc.*, 2004, **126**, 2688-2689; (c) E. L. Whitelaw, G. Loraine, M. F. Mahon and M. D. Jones, *Dalton Trans.*, 2011, **40**, 11469–11473; (d) A. Pilone, N. D. Maio, K. Press, V. Venditto, D. Pappalardo, M. Mazzeo, C. Pellecchia, M. Kol and M. Lamberti, *Dalton Trans.*, 2015, **44**, 2157-2165; (e) J.-C. Buffet and J. Okuda, *J. Polym. Chem.*, 2011, **28**, 275; (f) H.-L. Chen, S. Dutta, P.-Y. Huang and C.-C. Lin, *Organometallics*, 2012, **31**, 2016–2025; (g) T. R. Forder, M. D. Jones. New J. Chem., 2015, 39, 1974-78.

6 (a) P. Horeglad, G. Szczepaniak, M. Dranka and J. Zachara, Chem. Commun., 2012, **48**, 1171-1173; (b) S. Ghosh, R. R. Gowda, R. Jagan and D. Chakraborty, *Dalton Trans.*, DOI: 10.1039/c5dt00811e; (c) P. Horeglad, P. Kruk and J. Pécaut, Organometallics, 2010, **29**, 3729-3734.

7 (a) A.-F. Douglas, B. O. Patrick and P. Merkhodavandi, *Angew. Chem., Int., Ed.*, 2008, **47**, 2290–2293; (b) I. Peckermann, A. Kapelski, T. P. Spaniol and J. Okuda, *Inorg. Chem.*, 2009, **48**, 5526–5534; (c) D. C. Aluthge, B. O. Patrick and P. Mehrkhodavandi, *Chem. Commun.*, 2013, **49**, 4295–4297; (d) E. M. Broderick, N. Guo, C. S. Vogel, C. Xu, J. Sutter, J. T. Miller, K. Meyer, P. Mehrkhodavandi and P. L. Diaconescu, *J. Am. Chem. Soc.*, 2011, **133**, 9278–9281; (e) L. E. N. Allan, G. G. Briand, A. Decken, J. D. Marks, M. P. Shaver and R. G. Wareham, *J. Organomet. Chem.*, 2013, **736**, 55–62; (f) D. C. Aluthge, B. O. Patrick and P. Mehrkhodavandi, *Chem. Commun.*, 2012, **48**, 6806–6808; (g) N. Maudoux, T. Roisnel, V. Dorcet, J.-F. Carpentier and Y. Sarazin, *Chem. Eur. J.*, 2014, **20**, 1–18.

8 (a) A. K. Sutar, T. Maharana, S. Dutta, C. T. Chen and C. C. Lin, *Chem. Soc. Rev.*, 2010, **39**, 1724-1746; (b) B.-T. Ko and C.-C. Lin, *J. Am. Chem. Soc.*, 2001, **123**, 7973-7977; (c) Y. Huang, Y.-H. Tsai, W.-C. Hung, C.-S. Lin, W. Wang, J.-H. Huang, S. Dutta and C.-C. Lin, *Inorg. Chem.*, 2010, **49**, 9416-9425.

9 (a) C. A. Wheaton, P. G. Hayes and B. J. Ireland, *Dalton Trans.*, 2009, **25**, 4832-4846; (b) M.-L. Shueh, Y.-S. Wang, B.-H. Huang, C.-Y. Kuo and C.-C. Lin, *Macromolecules*, 2004, **37**, 5155-5162; (c) H.-Y. Tang, H.-Y. Chen, J.-H. Huang and C.-C. Lin, *Macromolecules*, 2007, **40**, 8855-8860; (d) L. Wang and H. Ma, *Macromolecules*, 2010, **43**, 6535-6537.

10 J. P. Davin, J. C. Buffet, T. P. Spaniol and J. Okuda, *Dalton Trans.*, 2012, **41**, 12612-12618.

11 (a) B. J. O'Keefe, L. E. Breyfogle, M. A. Hillmyer and W. B. Tolman, *J. Am. Chem. Soc.*, 2002, **124**, 4384-4393; (b) M. Stolt, K. Krasowska, M. Rutkowska, H. Janik, A. Rosling and A. Södergård, *Polym. Int.*, 2005, **54**, 362-368; (c) J. Chen, J. L. Gorczynski and C. L. Fraser, *Macromol. Chem. Phys.*, 2010, **211**, 1272-1279.

12 (a) S. Abbina and G. Du, *ACS Macro Lett.*, 2014, **3**, 689-692; (b) C.M. Silvernail, L. J. Yao, L. M. R. Hill, M. A. Hillmyer and W. B. Tolman, *Inorg. Chem.*, 2007, **46**, 6565-6574; (c) H.-Y. Chen, H.-Y. Tang and C.-C. Lin, *Macromolecules*, 2006, **39**, 3745-3752; (d) B.-H. Huang, C.-N. Lin, M.-L. Hsueh, T. Athar and C.-C. Lin, *Polymer*, 2006, **47**, 6622-6629; (e) D. J. Darensbourg and O. Karroonnirun, *Inorg. Chem.*, 2010, **49**, 2360-2371; (f) M. H. Chisholm, J. C. Gallucci and H. Zhen, *Inorg. Chem.*, 2001, **40**, 5051-5054.

13 (a) M. Save, M. Schappacher and A. Soum, *Macromol. Chem. Phys.*, 2002, **203**, 889–899; (b) I. Peckermann, A. Kapelski, T. P. Spaniol and J. Okuda, *Inorg. Chem.*, 2009, **48**, 5526-5534; (c) Y. Luo, W. Li, D. Lin, Y. Yao, Y. Zhang and Q. Shen, *Organometallics*, 2010, **29**, 3507-3514; (d) Z. J. Zhang, X. P. Xu, W. Y. Li, Y. M. Yao, Y. Zhang, Q. Shen and Y. J. Luo, *Inorg. Chem.*, 2009, **48**, 5715-5724; (e) M. Sinenkov, E. Kirillov, T. Roisnel, G. Fukin, A. Trifonov and J. F. Carpentier, *Organometallics*, 2011, **30**, 5509-5523.

14 (a) A. Stopper, K. Press, J. Okuda, I. Goldberg and M. Kol, *Inorg. Chem.*, 2014, **53**, 9140-9150; (b) A. Stopper, J. Okuda and M. Kol, *Macromolecules*, 2012, **45**, 698-704; (c) Y. Takashima, Y. Nakayama, K. Watanabe, T. Itono, N. Ueyama, A. Nakamura, H. Yasuda, A. Harada and J. Okuda, *Macromolecules*, 2002, **35**, 7538-7544; (d) T. K. Saha, B. Rajashekhar and D. Chakraborty, *RSC Adv.*, 2012, **2**, 307-318; (e) T. R. Forder, M. F. Mahon, M. G. Davidson, T. Woodman and M. D. Jones, *Dalton Trans.*, 2014, **43**, 12095-12099; (f) S. K. Roymuhury, D. Chakraborty and V. Ramkumar, *Dalton Trans.*, 2015, **44**, 10352-10367; (g) M. Mandal, D. Chakraborty and V. Ramkumar, *RSC Adv.,* 2015, **5**, 28536-28553; (h) S. L. Hancock, M. F. Mahon and M. D. Jones, *Chem. Cent. J.*, 2013, **7**, 135; (i) A. J. Chmura, D. M. Cousins, M. G. Davidson, M. D. Jones, M. D. Lunn and M. F. Mahon, *Dalton Trans.*, 2008, **11**, 1437-1443; (j) A. J. Chmura, M. G. Davidson, M. D. Jones, M. D. Lunn, M. F. Mahon, A. F. Johnson, P. Khunkamchoo, S. L. Roberts and S. S. F. Wong, *Macromolecules*, 2006, **39**, 7250-7257; (k) D. Chakraborty, D. Mandal, V. Ramkumar, V. Subramanian and J. V. Sundar, *Polymer*, 2015, **56**, 157-170; (l) R. C. J. Atkinson, K. Gerry, V. C. Gibson, N. J. Long, E. L. Marshall and L. J. West, *Organometallics*, 2007, **26**, 316–320; (m) C. Romain, B. Heinrich, S. B. Laponnaz and S. Dagorne, *Chem. Commun.*, 2012, **48**, 2213-2215; (n) B. Gao, Q. Duan, Y. Li, D. Li, L. Zhang, Y. Cui, N. Hu and X. Pang, *RSC Adv.*, 2015, **5**, 13437-13442; (o) H.-W. Ou, M. Y. Chiang, J. K. Vandavasi, W.-Y. Lu, Y.-J. Chen, H.-C. Tseng, Y.-C. Lai and H.-Y. Chen, *RSC Adv.*, 2015, **5**, 477-484.

15 (a) M. Zhang, X. Ni and Z. Shen, *Organometallics*, 2014, **33**, 6861-6867; (b) R. Stephen, R. B. Sunoj and P. Ghosh, *Dalton Trans.*, 2011, **40**, 10156-10161; (c) E. Kim, J. Jhang and J. S. Chung, *Macromol. Res.*, 2014, **22**, 864-869; (d) H. A. Brown, S. Xiong, G. A. Medvedev, Y. A. Chang, M. M. Abu-Omar, J. M. Caruthers and R. M. Waymouth, *Macromolecules*, 2014, **47**, 2955-2963; (e) E. Brulé, V. Guérineau, P. Vermaut, F. Prima, J. Balogh, L. Maron, A. M. Z. Slawin, S. P. Nolan and C. P. Thomas, *Polym. Chem.*, 2013, **4**, 2414-2423; (f) A. K. Acharya, Y. A. Chang, G. O. Jones, J. E. Rice, J. L. Hedrick, H. W. Horn and R. M. Waymouth, *J. Phys. Chem. B*, 2014, **118**, 6553-6560.

16 Y. Kim, P. N. Kapoor and J. G. Verkade, *Inorg. Chem.*, 2002, **41**, 4834–4838.

17 C. Alonso-Moreno, A. Antiñolo, J. C. García-Martínez, S. García-Yuste, I. López-Solera, A. Otero, J. C. Pérez-Flores and M. T. Tercero-Morales, *Eur. J. Inorg. Chem.*, 2012, 1139–1144.

18 T. K. Saha, M. Mandal, M. Thunga, D. Chakraborty and V. Ramkumar, *Dalton Trans.*, 2013, **42**, 10304-10314.

19 Y. Al-Khafaji, X. Sun, T. J. Prior, M. R. J. Elsegood and C. Redshaw, *Dalton Trans.*, 2015, **DOI:** 10.1039/C5DT00272A.

20 S. K. Roymuhury, D. Chakraborty and V. Ramkumar, *New J. Chem.*, 2015, **39**, 5218-5230.

View Article Online
DOI: 10.1039/C6RA09789H

21 M. M. Hännien, R. Sillanpää, H. Kivelä and A. Lehtonen, *Dalton Trans.*, 2011, **40**, 2868-2874.
22 (a) T. K. Saha, D. Chakraborty and V. Ramkumar, *Inorg. Chem.*, 2011, **50**, 2720-2722; (b) S. Gendler, S. Segal, I. Goldberg, Z. Goldschmidt and M. Kol, *Inorg. Chem.*, 2006, **45**, 4783-4790; (c) M. Grellier, L. Vendier, B. Chaudret, A. Albinati, S. Rizzato, S. Mason and S. Sabo-Etienne, *J. Am. Chem. Soc.*, 2005, **127**, 17592-17593; (d) S. Pappuru, E. R. Chokkapu, D. Chakraborty and V. Ramkumar, *Dalton Trans.*, 2013, **42**, 10304-10314;
23 G. A. Jeffrey, *An Introduction to Hydrogen Bonding*, Oxford University Press, New York, 1997.
24 J. Baran, A. Duda, A. Kowalski, R. Szymanski and S. Penczec, *Macromol. Rapid Commun.*, 1997, 18, 325-333.
25 C. M. Thomas, *Chem. Soc. Rev*., 2010, **39**, 165–173.
26 (a) Y. Wang, B. Liu, X. Wang, W. Zhao, D. Liu, X. Liu and D. Cui, *Polym. Chem*., 2014, **5**, 4580-4588; (b) M. Helou, O. Miserque, J.-M. Brusson, J.-F. Carpentier and S. M. Guillaume, *Chem. Eur. J*., 2008, **14**, 8772-8775.
27 (a) N. de Sousa Sousa, R. B. de Lima, A. L. P. Silva, A. A. Tanaka, A. B. F. da Silva and J. de Jesus Gomes Varela Júnior, *Comput. Theor. Chem*., 2015, **1054**, 93-99; (b) R. G. Pearson, Inorg. Chem., 1988, **27**, 734-740; (c) R. G. Parr and R. G. Pearson, J. Am. Chem. Soc., 1983, **105**, 7512-7516; (d) T. M. Pappenfus, B. J. Hermanson, T. J. Helland, G. G. W. Lee, S. M. Drew, K. R. Mann, K. A. McGee and S. C. Rasmussen, *Org. Lett*., 2008, **10**, 1553-1556.
28 D. B. G. Williams and M. Lawton, *J. Org. Chem*., 2010, **75**, 8351–8354.
29 G. M. Sheldrick, **SHELXL97**. *Program for crystal structure refinement*, Göttingen, Germany.
30 Gaussian 09, Revision C.01, M. J. Frisch, G. W. Trucks, H. B. Schlegel, G. E. Scuseria, M. A. Robb, J. R. Cheeseman, G. Scalmani, V. Barone, B. Mennucci, G. A. Petersson, H. Nakatsuji, M. Caricato, X. Li, H. P. Hratchian, A. F. Izmaylov, J. Bloino, G. Zheng, J. L. Sonnenberg, M. Hada, M. Ehara, K. Toyota, R. Fukuda, J. Hasegawa, M. Ishida, T. Nakajima, Y. Honda, O. Kitao, H. Nakai, T. Vreven, J. A. Montgomery, Jr., J. E. Peralta, F. Ogliaro, M. Bearpark, J. J. Heyd, E. Brothers, K. N. Kudin, V. N. Staroverov, T. Keith, R. Kobayashi, J. Normand, K. Raghavachari, A. Rendell, J. C. Burant, S. S. Iyengar, J. Tomasi, M. Cossi, N. Rega, J. M. Millam, M. Klene, J. E. Knox, J. B. Cross, V. Bakken, C. Adamo, J. Jaramillo, R. Gomperts, R. E. Stratmann, O. Yazyev, A. J. Austin, R. Cammi, C. Pomelli, J. W. Ochterski, R. L. Martin, K. Morokuma, V. G. Zakrzewski, G. A. Voth, P. Salvador, J. J. Dannenberg, S. Dapprich, A. D. Daniels, O. Farkas, J. B. Foresman, J. V. Ortiz, J. Cioslowski, and D. J. Fox, Gaussian, Inc., Wallingford CT, 2010.
31 C. G. Zhan, J. A. Nicholes and D. A. Dixon, *J. Phys. Chem. A*, 2003, **107**, 4184-4195.

View Article Online
DOI: 10.1039/C6RA09789H

Graphical Abstract: